Neutrophil IL-1β secretion induced by ExoS expressing *Pseudomonas aeruginosa* is dependent on NLRP3 and Gasdermin D

Martin S. Minns[1*], Tatiane S. Lima[1*], Karl Liboro[1*], Serena Abbondante[1], Michaela E. Marshall[1], Arne Rietsch[2], George R. Dubyak[3] and Eric Pearlman[1,4]

[1] Departments of Ophthalmology and Physiology & Biophysics, University of California, Irvine

[2] Department of Molecular Biology and Microbiology, and [3] Department of Physiology & Biophysics, Case Western Reserve University, Cleveland, OH

[4] Corresponding author (eric.pearlman@uci.edu)

*These authors contributed equally

ABSTRACT

Macrophages infected with Gram-negative bacteria expressing flagellin or Type III secretion system (T3SS) structural proteins are known to activate the NLRC4 inflammasome, resulting in caspase-1 and Gasdermin D (GSDMD) cleavage, IL-1β secretion and pyroptotic cell death. We examined the role of these mediators in IL-1β secretion by neutrophils infected with *Pseudomonas aeruginosa* strain PAO1 that expresses the Type III secretion system (T3SS) effectors ExoS and ExoT. We found that IL-1β secretion by neutrophils was dependent on expression of the T3SS needle and translocon proteins. Although pro-GSDMD and pro-GSDME were processed in PAO1 infected neutrophils, only GSDMD was required for IL-1β secretion. PAO1 – induced IL-1β secretion by macrophages was NLRC4 dependent, IL-1β secretion by neutrophils utilized NLRC4 only in the absence of *P. aeruginosa* exoenzymes. Instead, PAO1 – induced IL-1β secretion required NLRP3, which mediated by ExoS ADP ribosyl transferase activity. Overall, these findings reveal fundamental differences between neutrophils and macrophages in IL-1β secretion in response to pathogenic bacteria.

The discovery of the Gasdermin (GSDM) family of pore forming proteins has greatly increased our understanding of the mechanism of cell death in inflammation, cancer, and autoimmunity in addition to host defense, and has identified new targets for pharmacological interventions [1]. N-GSDMD forms pores in the plasma membrane of macrophages, leading to pyroptosis and release of mature IL-1β by pre-lytic mechanisms and/or in conjunction with pyroptotic lysis [1]. Compared with macrophages, there are relatively few studies examining the role of GSDMs in neutrophils, even though they vastly outnumber other cells recruited to sites of inflammation and infection, especially at early time points. We and others demonstrated that neutrophils are an important source of IL-1β [2, 3, 4, 5], and that secretion is dependent on GSDMD [6, 7].

P. aeruginosa is a ubiquitous environmental Gram-negative bacterium, and is an important cause of dermal, ocular and pulmonary disease, including cystic fibrosis. The Type III secretion system (T3SS) is a major virulence factor of *P. aeruginosa* that comprises an intricate needle structure that penetrates the plasma membrane of the target mammalian cell and injects exotoxins directly into the cytosol. Up to four effectors (exoezymes) are injected via the T3SS and have a variety of functions, including cell lysis by the phospholipase ExoU, or modulation of protein function by ADP ribosyl transferase (ADPRT) or GTPase activating protein (GAP) activities of ExoS and ExoT [8]. The nucleotidyl cyclase ExoY is also produced by ExoS expressing strains but has no recognized role in infection [9]. Our studies have focused on the role of blinding *P. aeruginosa* infections of the cornea (keratitis), which are a major cause of corneal ulcers in the USA and worldwide [10]. *P. aeruginosa* express either ExoS or ExoU, but rarely both, and most clinical isolates express ExoS and ExoT rather than ExoU [11, 12]. Using a murine model of keratitis driven by ExoS expressing bacteria, we reported that *P. aeruginosa* requires both an intact T3SS and the ADPRT activities of ExoS and ExoT for virulence [13]. We also showed that ExoS ADP-ribosylates the RAS small GTPase in neutrophils and blocks

assembly of the NADPH oxidase complex, resulting in lower ROS production and impaired bacterial killing [14].

Neutrophils comprise over 90% of the total cells in patients with corneal ulcers caused by *P. aeruginosa;* further, quantitative PCR analysis of ulcers revealed greatly elevated gene expression of IL-1β and the inflammasome proteins NLRC4, NLRP3 and ASC compared with uninfected human corneas [11]. Similarly, we found that >90% infiltrating cells in murine models of bacterial keratitis are neutrophils, and that these cells are the predominant source of IL-1β [2, 3, 4].

In contrast to macrophages, IL-1β secretion by neutrophils stimulated by canonical NLRP3 activators, *Streptococcus pneumoniae* or by *Salmonella* activation of NLRC4 occurs in the absence of pyroptotic cell death [3, 4, 5]. Canonical pyroptosis and IL-1β secretion in macrophages is driven by GSDMD, which is cleaved by caspase-1 to generate N-terminal subunits (N-GSDMD). Multiple N-GSDMD subunits insert into the inner leaflet of the plasma membrane where they form pores through which bioactive, cleaved IL-1β is secreted (reviewed in [15]). We reported that instead of inserting into the plasma membrane, N-GSDMD induced by ATP or nigericin localizes to neutrophil primary granules and autophagosomes. Further, N-GSDMD in primary granules resulted in release of neutrophil elastase (NE) into the cytosol, leading to NE cleavage of pro-GSDMD [7, 16, 17]. Differential roles for Gasdermin family proteins in neutrophils versus macrophages during inflammasome signaling has been further extended to GSDME. GSDME was first reported as a mutated gene (DFNA5) associated with hearing loss, but also forms plasma membrane pores following cleavage by caspase-3 (reviewed in [1]). Recently, the *Yersinia* T3SS acetyltransferase *YopJ* was found to activate GSDME rather than GSDMD to induce IL-1β secretion and cell death in neutrophils, but not in macrophages [18].

In the current study, we characterized the relative contributions of NLRP3, NLRC4, GSDMD and GSDME to inflammasome activation, IL-1β release, and pyroptosis in neutrophils versus macrophages following infection with T3SS expressing *P. aeruginosa.* Surprisingly, while

we found that the *P. aeruginosa* needle structure proteins were required for NLRC4 activation by macrophages as reported [19], ExoS ADP ribosyl transferase expression led to IL-1β secretion through the NLRP3 rather than the NLRC4 inflammasome in neutrophils. We also found no role for GSDME, and that although GSDMD was reported to mediate neutrophil extracellular trap formation (NETosis) induced by PMA or intracellular LPS [17, 20], we found that NETosis induced by PMA or *P. aeruginosa* was completely independent of GSDMD. Together, these findings underscore how particular components of inflammasome signaling networks are differentially engaged in neutrophils versus macrophages by the *P. aeruginosa* T3SS and specific injected effectors to modulate host response to clinically important strains of this microbial pathogen.

RESULTS

The P. aeruginosa T3SS needle and translocon structures mediate neutrophil pyroptotic IL-1β release through GSDMD

Canonical ATP induced activation of NLRP3 leading to IL-1β secretion in neutrophils is dependent on GSDMD but occurs in the absence of pyroptotic cell death [7]. To determine if there is a role for T3SS,GSDMD and GSDME in *P. aeruginosa* – induced IL-1β secretion by neutrophils, mouse bone marrow neutrophils from C57BL/6 mice were isolated by negative bead selection (>95% purity), incubated 3h with LPS to induce pro- IL-1β, and infected with *P. aeruginosa* for 60 min at an MOI of 30:1. **Figure 1A** shows the major proteins that comprise the *P. aeruginosa* T3SS, including the injectosome (the needle structure) and translocon pore in the host cell membrane that transport the effectors from the bacterial cytosol through the inner and outer membranes into the target eukaryotic cell. To examine the role of T3SS in IL-1β secretion, neutrophils were infected with strain PAO1 that expresses ExoS, T and Y, with Δ*pscD* (apparatus mutant), Δ*popB* (translocon mutant), or with exoenzyme mutants Δ*exoSTY* and Δ*exoST* that express the needle structure, but not the exoenzymes.

Pro-IL-1β was processed in neutrophils infected with *P. aeruginosa* strains PAO1, Δ*exoSTY* and Δ*exoST*, but not in neutrophils infected with the Δ*pscD* apparatus mutant or the Δ*popB* translocon mutant (**Figure 1B).** Consistent with this finding, only strains expressing the intact needle structure (PAO1, Δ*exoSTY* and Δ*exoST)* induced IL-1β secretion and pyroptotic cell death quantified by LDH release (**Figure 1C, D)**. Similar results were found in peritoneal neutrophils directly infected with these strains in the absence of LPS priming (data not shown).

To determine if there is a role for GSDMD or GSDME in IL-1β secretion following *P. aeruginosa* infection, neutrophils and macrophages from C57BL/6, *gsdmd*$^{-/-}$, *gsdme*$^{-/-}$ *and gsdmd / gsdme*$^{-/-}$ (double knockout) mice were infected with T3SS expressing PAO1 strain, and pro-GSDMD and pro-GSDME cleavage was identified by western blot. As a positive control for

caspase-3 and pro-GSDME cleavage, neutrophils and macrophages were stimulated with TNF-α plus second mitochondria-derived activator of caspases (SMAC) mimetic (SM), which activate the ripoptosome and apoptotic caspases [15]. Cells were stimulated in the presence of the pan-caspase inhibitor ZVAD or with cycloheximide, and macrophages were incubated in the presence of glycine to inhibit cell lysis. GM-CSF was added to neutrophil cultures to prevent spontaneous caspase-3 mediated apoptosis.

We found that in neutrophils and macrophages, PAO1 induced GSDMD cleavage that was inhibited with ZVAD, whereas caspase-3 cleavage was only detected following TNF/SM stimulation of the ripoptosome **(Figure 1E)**. GSDME cleavage was induced by PAO1 in neutrophils, but not in macrophages, and was not inhibited by ZVAD **(Figure 1F).** Taken together with absence of caspase-3 activation, PAO1 infected neutrophils appear to cleave GSDME by a caspase-independent mechanism.

To determine if GSDME is required for IL-1β secretion and cell death following infection with ExoS expressing *P. aeruginosa,* bone marrow neutrophils isolated from GSDMD$^{-/-}$, GSDME$^{-/-}$ and GSDMD/E$^{-/-}$ mice were primed with LPS and incubated 1h with ATP, PAO1, Δ*pscD* or Δ*exoST* mutant bacteria. We found that IL-1β secretion LDH release by neutrophils stimulated with ATP, PAO1 or Δ*exoST* mutants was significantly lower in GSDMD$^{-/-}$ and GSDMD/E$^{-/-}$ neutrophils compared with C57BL/6 neutrophils; however, there was no significant difference in IL-1β secretion between neutrophils from C57BL/6 and GSDME-/- mice **(Figure 1G, H)**. Similarly, IL-1β secretion and LDH release by macrophages was completely dependent on GSDMD **(Figure 1I, J)**.

Collectively, these findings demonstrate that *P. aeruginosa* induces IL-1β secretion and pyroptotic cell death in neutrophils, which is dependent on expression of the needle structure and the translocon. As Δ*exoST* mutants induced similar responses to wild type PAO1, we initially concluded that T3SS exotoxins are not required for IL-1β release. Further, although

PAO1 induces GSDME cleavage in neutrophils, there is no apparent role for GSDME in IL-1β secretion induced by T3SS expressing *P. aeruginosa*.

Neutrophil IL-1β secretion is NLRC4 independent during infection with ExoS/ExoT expressing P. aeruginosa

In macrophages, IL-1β secretion and pyroptosis induced by the needle structure and flagella of *P. aeruginosa* and other Gram-negative bacteria is mediated by NLRC4 [19, 21, 22, 23, 24]. As the intact needle structure was also required to for GSDMD cleavage and IL-1β secretion by neutrophils, we next examined the role of NLRC4 in IL-1β secretion by *P. aeruginosa.* Bone marrow neutrophils and bone marrow derived macrophages from C57BL/6 and NLRC4$^{-/-}$ mice were LPS primed and incubated with PAO1, or with Δ*pscD* or Δ*exoST* mutant bacteria, and IL-1β and LDH were quantified as before.

IL-1β secretion and LDH release by macrophages infected with PAO1 or the Δ*exoST* mutant was completely inhibited in the absence of NLRC4, whereas there was no difference between C57BL/6 and NLRC4$^{-/-}$ macrophages stimulated with the canonical NLRP3 activator ATP (**Figure 2A, B)**. Consistent with these findings, pro-GSDMD and pro-IL-1β cleavage was detected in lysates from C57BL/6 but not NLRC4$^{-/-}$ macrophages following incubation with *P. aeruginosa* PAO1 or the Δ*exoST* mutant (**Figure 2C)**. For western blot analysis, macrophages were stimulated in the presence of glycine to inhibit pyroptotic cell death [25, 26].

In contrast to macrophages, while IL-1β secretion and LDH release in neutrophils infected with Δ*exoST* mutants was NLRC4 dependent, NLRC4$^{-/-}$ neutrophils infected with wild-type PAO1 were not significantly different from C57BL/6 neutrophils (**Figure 2D, E**). Similarly, NLRC4 was required for GSDMD and IL-1β cleavage in neutrophils infected with Δ*exoST* mutants, but not with PAO1 (**Figure 2F).**

Collectively, these findings are consistent with earlier reports that *P. aeruginosa* induced IL-1β secretion by macrophages is dependent on NLRC4; however, we now show that in neutrophils infected with *P. aeruginosa* expressing ExoS and ExoT (PAO1), IL-1β secretion is NLRC4 independent.

Neutrophil IL-1β secretion is NLRP3 dependent during infection with ExoS/ExoT expressing P. aeruginosa due to selective mediation by the ExoS ADPRT

As NLRC4 is not required for IL-1β secretion in PAO1 infected neutrophils, we examined if ExoS and/or ExoT induce IL-1β secretion through the NLRP3 inflammasome. C57BL/6 and NLRP3$^{-/-}$ neutrophils and macrophages were incubated with either PAO1 or the Δ*exoST* mutant strain, and pro-GSDMD and pro-IL-1β cleavage and secretion were examined.

Consistent with the requirement for NLRC4 in IL-1β secretion by macrophages incubated with PAO1 or Δ*exoST,* there was no difference in IL-1β secretion or LDH release between C57BL/6 and NLRP3$^{-/-}$ macrophages (**Figure 3A, C).** In marked contrast, IL-1β secretion by NLRP3$^{-/-}$ neutrophils infected with PAO1 was significantly lower in compared with C57BL/6 mice, whereas there was no difference in neutrophils incubated with Δ*exoST* mutants **(Figure 3C)**. LDH release was also lower in NLRP3$^{-/-}$ mice, though the difference was not statistically significant **(Figure 3D**). These findings were reflected in western blot analysis that showed cleaved GSDMD and IL-1β in C57BL/6 but not NLRP3$^{-/-}$ infected with PAO1 whereas there was no difference in cleavage between C57BL/6 and NLRP3$^{-/-}$ neutrophils incubated with Δ*exoST* **(Figure 3E).**

As a second approach to examine the role of NLRP3, neutrophils from C57BL/6 mice were incubated with the well-characterized NLRP3 inhibitor MCC950 [27] prior to infection with *P. aeruginosa*. As with NLRP3$^{-/-}$ neutrophils, GSDMD and IL-1β cleavage was inhibited in MCC950 treated neutrophils following infection with PAO1, but there was no effect of MCC950 in

neutrophils infected with the Δ*exoST* strain (**Figure 3F)**. Taken together with the observations of NLRC4$^{-/-}$ neutrophils, these findings demonstrate that ExoS and/or ExoT mediate activation of the NLRP3 instead of the NLRC4 inflammasome. Conversely, the T3SS needle apparatus activates the NLRC4 inflammasome.

P. aeruginosa ExoS and ExoT are bifunctional exotoxins with both GAP and ADPRT enzymatic activities (**Figure 3G)**. To identify which of these functions in ExoS and ExoT mediate NLRP3 dependent IL-1β secretion, bone marrow neutrophils from C57BL/6 were infected with PAO1 mutants that have point mutations in the enzymatic region of either the GAP or ADPRT domains of ExoS or ExoT in the presence of MCC950.

IL-1β secretion by PAO1 infected neutrophils was inhibited by MCC950, whereas there was no difference in neutrophils incubated with Δ*exoST* bacteria **(Figure 3H)**, which replicates our findings using NLRP3-/- neutrophils. Point mutations in GAP domains of ExoS and ExoT (*exoST(G-)*) or in the ExoT ADPRT domain (*exoT(A-)*) also phenocopied PAO1 in showing MCC950 inhibition (NLRP3 activity) whereas point mutations inactivating both ExoS and ExoT ADPRT domains (*exoST(A-)*), or the ExoS ADPRT domain (*exoS(A-)*) phenocopied the Δ*exoST* mutant strain in showing no effect of MCC950 (**Figure 3H)**. We also found that IL-1β production by neutrophils was inhibited in the presence of DPI, and was completely inhibited when incubated with MCC950 and DPI, but only in ExoS ADPRT producing strains (data not shown).

Taken together, these findings identify a requirement for the ADP ribosyltransferase activity of ExoS to induce NLRP3 rather than NLRC4 inflammasome activation in neutrophils.

NETosis induced by P. aeruginosa is dependent on expression of the needle structure, and is ROS, GSDMD and GSDME independent

Although *P. aeruginosa* induced neutrophils exhibit <30% LDH release, neutrophils also undergo cell death following a programmed release of nuclear DNA (neutrophil extracellular

traps, NETosis) following protein kinase C (PKC) activation of neutrophils by phorbol myristate acetate (PMA) or after incubation with bacteria and fungi [28, 29]. NETs contain nuclear DNA, histones and neutrophil proteases, and antimicrobial peptides that have antimicrobial and cytotoxic activities. GSDMD was reported to mediate NETosis induced by PMA or intracellular *Salmonella, Citrobacter* or transfected LPS [17, 20]. As *P. aeruginosa* induces NETosis in murine models of pulmonary and corneal infections [30, 31], we examined if there is a role for GSDMD or GSDME in NETosis induced by *P. aeruginosa*.

PMA induced NETosis in human neutrophils is dependent on production of reactive oxygen species (ROS) [28], and *P. aeruginosa* ExoS inhibits ROS production by human and murine neutrophils [14], and (**Figure S1A, B)**, we first examined if ROS is required for *P. aeruginosa* – induced NETosis. Human peripheral blood neutrophils were incubated with PAO1 or Δ*pscD* injectosome mutants together with the ROS inhibitor DPI, and total nucleic acid, including extracellular DNA was quantified using Sytox™ Green. Although PMA - induced NETosis was completely inhibited by DPI, there was no significant reduction in *P. aeruginosa* – induced NETosis in the presence of DPI (**Figure 5A-C)**, indicating a mechanistic difference between PMA and bacterial induced NETosis in human neutrophils. There was also significantly less extracellular DNA release from neutrophils incubated with Δ*pscD* mutant bacteria, indicating that the T3SS is required to induce NETosis (**Figure 5C)**.

To determine if there is a role for GSDMD in *P. aeruginosa* - mediated NETosis, neutrophils from the peritoneal cavity of C57BL/6 or GSDMD$^{-/-}$ mice were infected with PAO1 at a ratio of 30:1 and extracellular DNA assayed by increased Sytox green fluorescence was quantified over 16h. We found no significant difference in DNA release by neutrophils from GSDMD$^{-/-}$ compared with C57BL/6 mice following incubation with either PAO1 or PMA (**Figure 5D-F)**. As a second approach to examine the role of GSDMD in PAO1-induced NETosis, neutrophils from C57BL/6 mice were incubated with the LDC7559 that was reported to inhibit GSDMD-dependent NETosis [17], or with two other known GSDMD inhibitors, necrosulfonamide

(NSA) and disulfiram [32, 33]. There was a significant reduction in IL-1β secretion by neutrophils in the presence of NSA or disulfiram (but not LDC7559); however, there was no effect on NET formation (**Figure 5G, H).** There was also no difference in NET formation between neutrophils from C57BL/6 and GSDME$^{-/-}$ mice (**Figure 5I, J)**.

PMA - induced NETosis is mediated by protein deiminase 4 (PAD4), which contributes to histone citrullination and chromatin decondensation during NETosis [34]. Using antibodies to citrullinated histone 3 (H3Cit) we found histone citrullination in neutrophils stimulated with PMA or *P. aeruginosa* strain PAO1; however, there was no difference between neutrophils from C57BL/6 and GSDMD$^{-/-}$ mice (**Figure 5K, L).** Lower magnification images are in **Figure S1C).**

Redundant roles for GSDMD and GSDME in P. aeruginosa infection in vivo

We reported that *P. aeruginosa* killing in infected corneas (keratitis) was dependent on neutrophils, IL-1β, and on Type III secretion [2, 13, 14, 35]. To determine if there is a requirement for GSDMD or GSDME *in vivo*, we used a well-established murine model of blinding *P. aeruginosa* keratitis. Corneas of C57BL/6 and GSDMD/GSDME-/- mice were abraded and infected with PAO1, and after 24h when neutrophil infiltration was maximal, we dissected and homogenized corneas, and examined GSDMD, GSDME and IL-1β cleavage by western blot.

N-GSDMD, N-GSDME and cleaved IL-1β were detected in PAO1 infected C57BL/6 corneas, and IL-1β cleavage was impaired in GSDMD/ GSDME$^{-/-}$ compared with C57BL/6 corneas (**Figure 5A)**. However, there was no difference in total IL-1β or CFU between C57BL/6 and either *gsdmd*$^{-/-}$ or *gsdmd* / *gsdme* $^{-/-}$ mice (**Figure 5B).** There was also no difference in corneal opacification among these mouse strains (**Fig S2)**.

DISCUSSION

Bacterial T3SS effectors are efficiently injected into target eukaryotic cells where they can compromise the host immune response. For example, recent studies show that the *Shigella flexneri* T3SS ubiquitin ligase IpaH7.8 selectively targets human GSDMB and GSDMD for proteasomal degradation, thereby inhibiting GSDMB mediated bacterial killing, or inhibiting GSDMD mediated host cell lysis and protecting the replicative environment [36, 37]. *Pseudomonas, Salmonella,* and *Yersinia* T3SS and *Legionella* Type IV secretion activate IL-1β secretion and pyroptosis by macrophages primarily through recognition of needle structure proteins by NAIP1 and NAIP2 (humans have a single NAIP [38]) and activation of the NLRC4 inflammasome [19]. *Yersinia YopJ* acetyltransferase promotes macrophage pro-IL-1β and GSDMD cleavage and pyroptosis [39, 40].

In contrast to macrophages, there are relatively few reports on the role of neutrophils as a source of IL-1β during bacterial infection. In *Burkholderia* infected neutrophils, IL-1β secretion and pro-GSDMD cleavage by neutrophils requires caspase-1 or caspase-11, and selective deletion of caspase-11 in neutrophils resulted in impaired bacterial killing [41]. Further, survival of mice infected with *YopJ* expressing *Yersinia* was dependent on GSDME rather than GSDMD, and GSDME was required for IL-1β secretion by neutrophils rather than macrophages [18]. Consistent with that report, we found that *P. aeruginosa* induces pro-GSDME cleavage only in neutrophils; however, IL-1β secretion was dependent on GSDMD rather than GSDME. Further, while pro-GSDME is known to be cleaved by caspase-3 [15], we found that pro-caspase-3 was not cleaved in *P. aeruginosa* infected neutrophils. As we and others reported that serine proteases such as neutrophil elastase can cleave pro-GSDMD [7, 16, 17], it is possible that in neutrophils, serine proteases also cleave pro-GSDME.

The differences in the host and bacterial mediators of IL-1β secretion between macrophages and neutrophils infected with *P. aeruginosa* are summarized in **Figure 6.** Pre-

incubation with LPS induces expression of pro- IL-1β in macrophages and neutrophils; however, following macrophage infection with T3SS expressing *P. aeruginosa,* the needle and translocon structures selectively activate NLRC4 (through NAIP1 and NAIP2), resulting in caspase-1 mediated IL-1β and GSDMD cleavage, plasma membrane pore formation, pyroptosis and secretion of bioactive IL-1β. While these findings are consistent with earlier reports using *P. aeruginosa* [19, 24, 42], we also found no apparent role for bacterial exoenzymes in this process as exoenzyme expressing bacteria also activated NLRC4. In contrast, while the needle structure activated NLRC4 in neutrophils in the absence of exoenzymes (in Δ*exoST* mutants), leading to cleavage of GSDMD and IL-1β, in the presence of ExoS and ExoT, NLRP3 rather than NLRC4 was required for the pro-GSDMD and IL-1β cleavage. We identified ExoS ADPRT as the mediator of selective NLRP3 activation.

The underlying differences in inflammasome dependence between neutrophils and macrophages are unclear, although as macrophages produce more caspase-1 and caspase-11 than neutrophils on a per cell basis [20, 43], it is possible that macrophages produce more NAIPs or NLRC4 than neutrophils, resulting in more rapid NLRC4 mediated responses in macrophages. However, despite the *P. aeruginosa* needle structure activating NLRC4 in neutrophils, we found IL-1β secretion induced by ExoS expressing strains to be entirely NLRP3 dependent. NLRP3 may also be a substrate for ExoS ADPRT, resulting in increased activity. Gain of function mutations in NLRP3 are the cause of cryopyrin associated period syndromes (CAPS) [44]. Neutrophils are the major source of IL-1β in CAPS patients, and gain of function mutations expressed only in neutrophils are sufficient to induce CAPS like symptoms in mice [45]. NLRP3 activity is also regulated by post-translational modifications, including JNK phosphorylation of NLRP3, which initiates aggregation during LPS priming [46]. Enzymes that regulate ubiquitylation and deubiquitylation also regulate NRLP3 activity [47, 48]. This includes the *Mycoplasma pneumoniae* community-acquired respiratory distress syndrome (CARDS) toxin that ADP

ribosylates NLRP3 [49, 50]. In another study, macrophages incubated with recombinant CARDS toxin induced IL-1β secretion through NLRP3, the ADPRT enzymatic activity was required, and CARDS toxin interacted with NLRP3 [49], implying that ADP ribosylation resulted in increased NLRP3 activity. Similarly, Group A Streptococcus *SpyA* ribosyl transferase toxin induced NLRP3/caspase-1 dependent IL-1β secretion by macrophages, although these investigators did not examine inflammasome usage [51].

An alternate mechanism is that ExoS ADPRT targets other proteins involved in inflammasome activity, possibly inhibiting NAIP or NLRC4, which remain inactive even in the absence of NLRP3. Although most reports cite modifications that enhance NLRC4 activity [52, 53], future studies will examine the possibility of inhibiting this pathway. Taken together with results from the current study, it seems more likely that ExoS activates NLRP3 in neutrophils, which will be examined in future studies. An important caveat in performing these experiments is that ExoS ADPRT is highly promiscuous, and has multiple substrates [8]. In support of this concept, a recent report showed that expression of ExoS ADPRT correlated with decreased lytic cell death in corneal epithelial cells [54], although the target proteins were not identified.

We reported that activation of the NLRP3 inflammasome in neutrophils by *Streptococcus pneumoniae* or ATP does not lead to pyroptotic cell death as quantified by LDH release [3, 4, 7]. Here we find that T3SS expressing *P. aeruginosa* induce LDH release (~30% of triton control), which is lower than for macrophages. We also found that the T3SS is required for *P. aeruginosa* induced NETosis, which can also lead to IL-1β release. *P. aeruginosa* induced NETosis was ROS-independent, but involved histone 3 citrullination. While a prior report showed a requirement for GSDMD in PMA – induced NETosis [17], we found that GSDMD had no apparent role in PMA or *P. aeruginosa* induced NETosis when quantified by Sytox or H3Cit and using either GSDMD-/- neutrophils or GSDMD chemical inhibitors. Further, the inhibitor used in that study (LDC7559) was found to block the oxidative burst rather than GSDMD [55], although the

difference between their findings using GSDMD mutant mice[17] and ours has yet to be determined.

Finally, whereas GSDMD and GSDME were cleaved in *P. aeruginosa* infected corneas, there was no effect on bacterial killing or corneal disease in GSDMD$^{-/-}$ or GSDMD/GSDME$^{-/-}$ mice. Given that IL-1β-/- mice exhibit impaired *P. aeruginosa* killing in the cornea [2](and Supplemental Figure 3), that GSDMD is required for IL-1β secretion by neutrophils and macrophages, and there is less cleaved IL-1β in corneas of infected GSDMD/E-/- mice, we anticipated finding a difference in disease outcome. However, given the complexity of the inflammatory response in infected tissues, alternate pathways, such as neutrophil elastase-mediated in IL-1β cleavage [2], could explain the observed redundancy of GSDMD and GSDME *in vivo*.

Overall, results from the current study increase our understanding of the role of inflammasomes and GSDMs in neutrophils compared with macrophages, and also identify a novel role for *P. aeruginosa* T3SS.

Funding: Studies were supported by NIH grants R01-EY14362, R21-EY032662 (EP, GRD), R01-EY022052 and R21-AI153754 (AR). KL was supported by NIH T32AI141346. The authors acknowledge departmental support from an unrestricted grant to the Department of Ophthalmology from the Research to Prevent Blindness Foundation, New York, NY.

Data availability: The authors declare that data supporting the findings of the current study are available within the article and Supplementary Information or available from the corresponding authors upon request.

Author contributions: MM, TL and KL designed and performed in vitro experiments and MM, KL, SA and MM performed the *in vivo* experiments. MM, TL, KL, GRD AR, and EP wrote the manuscript.

Competing interests: The authors declare that they have no competing interests.

METHODS

Reagents

All reagents and antibodies are listed in Supplementary Table 1.

Source of mice

C57BL/6, *gsdme*$^{-/-}$ and *nlrp3*$^{-/-}$ mice were purchased from Jackson Laboratories. *Gsdmd*$^{-/-}$ and *nlrc4*$^{-/-}$ mice were a kind gift from Dr. Russell Vance (University of California, Berkeley). *Gsdmd*$^{-/-}$*gsdme*$^{-/-}$ mice were generated in-house. All transgenic mice were on a C57BL/6 background. Animals were housed in pathogen free conditions in microisolator cages and were treated according to institutional guidelines following approval by the University of California IACUC.

Bacterial culture

DMSO stocks of PAO1F and T3SS mutant strains were grown overnight in modified high salt LB (HSLB) broth containing 200 mM NaCl, 10 mM MgCl2, 0.5 mm CaCl2, and 5 mM EGTA to induce T3SS expression [56]. For experiments, overnight cultures were diluted 1:100 in fresh HSLB broth and grown to early log phase, OD_{600} of 0.18-0.2. Bacteria were washed in PBS, resuspended at $3x10^8$ bacteria/mL, and 20uL containing $6x\ 10^6$ bacteria were added to 200,000 neutrophils (MOI of 30) for *in vitro* stimulations.

Isolation of human blood neutrophils

Whole blood was collected from volunteers ages 18 and 65 years as part of the healthy blood donor program that is run by the Institute for Clinical and Translational Science at UC Irvine. This program has been approved by Institutional Review Board of the University of California (Irvine, CA), following informed consent, and donors were de-identified. Neutrophils were isolated using by density gradient centrifugation (Ficoll-Paque Plus, GE Healthcare) at 500 × *g* for 30 min, which yields >90% purity as assessed by flow cytometry using anti-human CD16 and CD66b Abs (eBiosciences).

Isolation of murine bone marrow and peritoneal neutrophils

Peritoneal neutrophils were elicited by injecting mice IP with 1 mL of a 9% casein solution for 16-20h followed by a second injection of casein 3h prior to collection. Peritoneal cells were drawn into cold PBS. Bone marrow neutrophils were collected from the tibia and femur of mice. Peritoneal or bone marrow neutrophils were enriched via negative selection magnetic beads using the manufacturer's recommended protocols (Biolegend MojoSort or STEMCELL EasySep), yielding >95% purity as determined by flow cytometry using antibodies to Ly6G and CD11b. Neutrophils were resuspended in RPMI (Gibco) at the specified concentrations for *in vitro* assays.

Generation of murine bone marrow derived macrophages

Bone marrow derived macrophages (BMDMs) were collected by seeding bone marrow into untreated culture flasks (Gen Clone, 25-214) containing 10 mL Dulbecco's modified Eagle's medium (DMEM; Gibco), 10% fetal bovine serum (FBS; Corning), and 10 ng/mL M-CSF (R&D Systems). On Day 2 and Day 4, non-adherent cells were removed by washing, and growth medium was replaced. On Day 6, BMDMs were detached using Cellstripper™ (Corning, NY) following manufacturer's directions and plated in media with 20 ng/mL GM-CSF (STEMCELL) for *in vitro* assays the following day.

GSDMD and GSDME stimulation and inhibition

Ultrapure lipopolysaccharide (LPS) (Invivogen) was used at 500 ng/mL for 3 h, and ATP (Sigma-Aldrich) was used at 3 mM for 1 h to selectively activate NLRP3. Recombinant TNFα (R&D Systems) at 100 ng/mL together with 2 μM Birinapant Smac mimetic (MedChemExpress) or 2.5 ng/mL cycloheximide (final concentrations) were added for 4h to induce caspase-3 and GSDME activation. The pan caspase inhibitor Z-VAD-FMK (APExBIO), the NLRP3 inhibitor

MCC950 (Invivogen) and the ROS inhibitor diphenyleneiodonium chloride (DPI, Sigma) were dissolved in dimethyl sulfoxide (DMSO) (Thermo Fisher Scientific). Cells were pretreated with ZVAD at 50 μM for 30 min, with MCC920 at 2 μM for 40 min, with DPI at 10 μM for 20 min, or with the equivalent volume of DMSO for a vehicle control. Cells were incubated with *Pseudomonas aeruginosa* strains at an MOI=30 for 25 min for western blots or 1h for cytokine production and LDH release. Neutrophils were suspended in media containing 20 ng/mL GM-CSF to reduce spontaneous activation of Caspase-3. Macrophages were pretreated with 5 mM glycine for 30 min to inhibit macrophage pyroptosis as described [25, 26].

Western Blot Analysis

After treatment, cells ($4x10^6$ BMNs or $2x10^6$ BMDMs) were lysed in 1x lysis buffer (CST). For neutrophils, we included 5 mM diisopropylfluorophosphate (DFP), which is a covalent inhibitor of neutral serine proteases such as neutrophil elastase. We found that DFP inhibits post-lysis processing of neutrophil proteins, including GSDMD [7]. Protein in 1-1.5 mL of supernatants was precipitated using 10% sodium deoxycholate and 100% TCA. The resulting pellets were washed with 100% acetone and resuspended in 0.2 M NaOH. BCA assays were run to determine protein concentrations, and 10-30 μg total protein in 1-1.5 mL of TCA-precipitated supernatant was separated on 4-20% acrylamide gels via SDS-PAGE. Protein was transferred to PVDF membranes (Millipore) using the TransBlot Turbo semi-dry apparatus (Bio-Rad).

Antibodies for western blot were diluted as follows: anti-IL-1β (1:800), anti- β -actin (1:500), anti-GSDMD (1:1000), anti-GSDME (1:1000), anti-caspase-3 (1:1000), HRP-conjugated secondary antibodies (1:1000). Membranes were developed using Supersignal West Femto Maximum Sensitivity Substrate (Thermo Scientific).

ELISA and cytotoxicity assays

Neutrophils ($2x10^5$ /well) or macrophages ($3.5x10^4$ /well) were stimulated as indicated. Cell-free supernatants were collected by centrifugation in V-bottom 96-well plates (PlateOne). Proteins were measured by ELISA following manufacturer's recommendations (DuoSet, R&D). Cell cytotoxicity was determined by quantifying LDH release with CytoTox 96® Non-Radioactive Cytotoxicity Assay (Promega) according to the manufacturer's instructions. Percentage cytotoxicity was calculated based on maximum LDH release.

Reactive oxygen species (ROS) quantification

Neutrophils were incubated with 50 μM luminol (Sigma) at $1x10^6$ cells/mL. Cells were plated in black-wall 96-well plates with an optically clear bottom (CoStar 3720) at $2x10^5$ neutrophils per well and incubated for 20-30 minutes. *P. aeruginosa* strains grown to log phase or other stimuli were added at indicated concentrations. Cells were incubated in the Cytation5 (BioTek) at 37°C and luminescence was measure from each well every 2 min for 90 min. Area under the curve was calculated using Prism (Graphpad).

NETosis assays

Sytox™ kinetic assay for extracellular DNA. Enriched neutrophils were resuspended at $1x10^6$ cells/mL in RPMI with 20 ng/mL GM-CSF (R&D or STEMCELL) (for murine neutrophils) or RPMI with 2% FBS (for human neutrophils) with 1 μM Sytox Green (Invitrogen) and plated in 96-well plates at 200,000 neutrophils per well. Log phase *P. aeruginosa* and other stimuli were added at indicated concentrations, and fluorescence (485 Ex/525 Em) was quantified every 15 min for 16h using a Cytation5 (BioTek) at 37°C with 5% CO2. The area under the curve between time 0- 6h was calculated using Prism (Graphpad).

NETosis detected by immunofluorescence. Enriched casein-elicited peritoneal mouse neutrophils were resuspended in RPMI with 20 ng/mL GM-CSF (R&D or STEMCELL) at $1x10^6$ cells/mL. 500,000 neutrophils were seeded onto sterile 12mm circular glass coverslips (#1.5, Thermo or EMS) in 24-well plates and stimulated as indicated. Coverslips were washed gently with cold PBS and fixed for 20 minutes at 4°C in 2% PFA in PBS. For washes and fixation, $CaCl_2$ and $MgCl_2$ were added to PBS at 0.9 mM and 0.5 mM, respectively. Coverslips were incubated for 1h in 10% normal donkey serum in PBS with 0.1% Triton X-100 and incubated overnight with indicated primary antibodies in blocking buffer. Coverslips were then washed in PBS, incubated in secondary antibodies for 2h, and counterstained in 0.1 µg/mL DAPI before being mounted to slides using VectaSHIELD HardSet (Vector Labs) and sealed with nail polish. Neutrophils were imaged using an LSM700 confocal microscope (Zeiss) and processed with FIJI/ImageJ (NIH) or Zen 2 blue edition (Zeiss).

Corneal infection model

Overnight cultures of *P. aeruginosa* PAO1F or indicated mutant strains were grown to log phase (OD_{600} of 0.2) in LB broth, then washed and resuspended in PBS at $5x10^7$ bacteria/mL. C57BL/6 and transgenic mice 7-12 weeks old were anesthetized with ketamine/xylazine solution, the corneal epithelium was abraded with three parallel scratches using a sterile 26-gauge needle, and 2 µL of bacteria were added topically (approximately $1x10^5$ bacteria per eye). Following infection, mice were euthanized and whole eyes in PBS were homogenized for CFU quantification using a TissueLyser II (Qiagen, 30 Hz for 3 minutes). CFU was also determined at 2 h to confirm the inoculum. Homogenates were serially diluted and streaked on LB plates for CFU quantification. For western blot and cytokine analyses, corneas were carefully dissected to remove vascularized iris tissue, and placed in 1x lysis buffer (CST) containing 5 mM DFP. Corneal opacity and corneal fluorescent intensity images were quantified using Image J software (NIH).

Statistics

Statistical significance was determined using unpaired t-test or two-way ANOVA with either HSD Tukey's post hoc analysis. For *in vivo* experiments, significance was determined using Student's t test (GraphPad Prism). Differences were considered significant when the *P* value was <0.05.

References

1. Liu X, Xia S, Zhang Z, Wu H, Lieberman J. Channelling inflammation: gasdermins in physiology and disease. *Nat Rev Drug Discov* **20**, 384-405 (2021).

2. Karmakar M, Sun Y, Hise AG, Rietsch A, Pearlman E. Cutting edge: IL-1beta processing during Pseudomonas aeruginosa infection is mediated by neutrophil serine proteases and is independent of NLRC4 and caspase-1. *J Immunol* **189**, 4231-4235 (2012).

3. Karmakar M, Katsnelson MA, Dubyak GR, Pearlman E. Neutrophil P2X7 receptors mediate NLRP3 inflammasome-dependent IL-1beta secretion in response to ATP. *Nat Commun* **7**, 10555 (2016).

4. Karmakar M*, et al.* Neutrophil IL-1beta processing induced by pneumolysin is mediated by the NLRP3/ASC inflammasome and caspase-1 activation and is dependent on K+ efflux. *J Immunol* **194**, 1763-1775 (2015).

5. Chen KW*, et al.* The neutrophil NLRC4 inflammasome selectively promotes IL-1beta maturation without pyroptosis during acute Salmonella challenge. *Cell Rep* **8**, 570-582 (2014).

6. Monteleone M*, et al.* Interleukin-1beta Maturation Triggers Its Relocation to the Plasma Membrane for Gasdermin-D-Dependent and -Independent Secretion. *Cell Rep* **24**, 1425-1433 (2018).

7. Karmakar M*, et al.* N-GSDMD trafficking to neutrophil organelles facilitates IL-1beta release independently of plasma membrane pores and pyroptosis. *Nat Commun* **11**, 2212 (2020).

8. Hauser AR. The type III secretion system of Pseudomonas aeruginosa: infection by injection. *Nat Rev Microbiol* **7**, 654-665 (2009).

9. Munder A*, et al.* The Pseudomonas aeruginosa ExoY phenotype of high-copy-number recombinants is not detectable in natural isolates. *Open Biol* **8**, (2018).

10. Ung L, Bispo PJM, Shanbhag SS, Gilmore MS, Chodosh J. The persistent dilemma of microbial keratitis: Global burden, diagnosis, and antimicrobial resistance. *Surv Ophthalmol* **64**, 255-271 (2019).

11. Karthikeyan RS*, et al.* Host response and bacterial virulence factor expression in Pseudomonas aeruginosa and Streptococcus pneumoniae corneal ulcers. *PLoS One* **8**, e64867 (2013).

12. Borkar DS*, et al.* Association between cytotoxic and invasive Pseudomonas aeruginosa and clinical outcomes in bacterial keratitis. *JAMA Ophthalmol* **131**, 147-153 (2013).

13. Sun Y, Karmakar M, Taylor PR, Rietsch A, Pearlman E. ExoS and ExoT ADP ribosyltransferase activities mediate Pseudomonas aeruginosa keratitis by promoting neutrophil apoptosis and bacterial survival. *J Immunol* **188**, 1884-1895 (2012).

14. Vareechon C, Zmina SE, Karmakar M, Pearlman E, Rietsch A. Pseudomonas aeruginosa Effector ExoS Inhibits ROS Production in Human Neutrophils. *Cell Host Microbe* **21**, 611-618 e615 (2017).

15. Broz P, Pelegrin P, Shao F. The gasdermins, a protein family executing cell death and inflammation. *Nat Rev Immunol* **20**, 143-157 (2020).

16. Kambara H*, et al.* Gasdermin D Exerts Anti-inflammatory Effects by Promoting Neutrophil Death. *Cell Rep* **22**, 2924-2936 (2018).

17. Sollberger G*, et al.* Gasdermin D plays a vital role in the generation of neutrophil extracellular traps. *Sci Immunol* **3**, (2018).

18. Chen KW*, et al.* RIPK1 activates distinct gasdermins in macrophages and neutrophils upon pathogen blockade of innate immune signaling. *Proc Natl Acad Sci U S A* **118**, (2021).

19. Miao EA*, et al.* Innate immune detection of the type III secretion apparatus through the NLRC4 inflammasome. *Proc Natl Acad Sci U S A* **107**, 3076-3080 (2010).

20. Chen KW*, et al.* Noncanonical inflammasome signaling elicits gasdermin D-dependent neutrophil extracellular traps. *Sci Immunol* **3**, (2018).

21. Zhao Y*, et al.* The NLRC4 inflammasome receptors for bacterial flagellin and type III secretion apparatus. *Nature* **477**, 596-600 (2011).

22. Zhao Y, Shao F. The NAIP-NLRC4 inflammasome in innate immune detection of bacterial flagellin and type III secretion apparatus. *Immunol Rev* **265**, 85-102 (2015).

23. Vance RE. The NAIP/NLRC4 inflammasomes. *Curr Opin Immunol* **32**, 84-89 (2015).

24. Sutterwala FS, Mijares LA, Li L, Ogura Y, Kazmierczak BI, Flavell RA. Immune recognition of Pseudomonas aeruginosa mediated by the IPAF/NLRC4 inflammasome. *J Exp Med* **204**, 3235-3245 (2007).

25. Evavold CL, Ruan J, Tan Y, Xia S, Wu H, Kagan JC. The Pore-Forming Protein Gasdermin D Regulates Interleukin-1 Secretion from Living Macrophages. *Immunity* **48**, 35-44 e36 (2018).

26. Loomis WP, den Hartigh AB, Cookson BT, Fink SL. Diverse small molecules prevent macrophage lysis during pyroptosis. *Cell Death Dis* **10**, 326 (2019).

27. Coll RC*, et al.* A small-molecule inhibitor of the NLRP3 inflammasome for the treatment of inflammatory diseases. *Nat Med* **21**, 248-255 (2015).

28. Fuchs TA*, et al.* Novel cell death program leads to neutrophil extracellular traps. *J Cell Biol* **176**, 231-241 (2007).

29. Brinkmann V*, et al.* Neutrophil extracellular traps kill bacteria. *Science* **303**, 1532-1535 (2004).

30. Skopelja-Gardner S*, et al.* Regulation of Pseudomonas aeruginosa-Mediated Neutrophil Extracellular Traps. *Front Immunol* **10**, 1670 (2019).

31. Thanabalasuriar A*, et al.* Neutrophil Extracellular Traps Confine Pseudomonas aeruginosa Ocular Biofilms and Restrict Brain Invasion. *Cell Host Microbe* **25**, 526-536 e524 (2019).

32. Rathkey JK*, et al.* Chemical disruption of the pyroptotic pore-forming protein gasdermin D inhibits inflammatory cell death and sepsis. *Sci Immunol* **3**, (2018).

33. Hu JJ*, et al.* FDA-approved disulfiram inhibits pyroptosis by blocking gasdermin D pore formation. *Nat Immunol* **21**, 736-745 (2020).

34. Sollberger G, Tilley DO, Zychlinsky A. Neutrophil Extracellular Traps: The Biology of Chromatin Externalization. *Dev Cell* **44**, 542-553 (2018).

35. Sun Y*, et al.* TLR4 and TLR5 on corneal macrophages regulate Pseudomonas aeruginosa keratitis by signaling through MyD88-dependent and -independent pathways. *J Immunol* **185**, 4272-4283 (2010).

36. Hansen JM*, et al.* Pathogenic ubiquitination of GSDMB inhibits NK cell bactericidal functions. *Cell* **184**, 3178-3191 e3118 (2021).

37. Luchetti G*, et al.* Shigella ubiquitin ligase IpaH7.8 targets gasdermin D for degradation to prevent pyroptosis and enable infection. *Cell Host Microbe* **29**, 1521-1530 e1510 (2021).

38. Bauer R, Rauch I. The NAIP/NLRC4 inflammasome in infection and pathology. *Mol Aspects Med* **76**, 100863 (2020).

39. Sarhan J*, et al.* Caspase-8 induces cleavage of gasdermin D to elicit pyroptosis during Yersinia infection. *Proc Natl Acad Sci U S A* **115**, E10888-E10897 (2018).

40. Orning P*, et al.* Pathogen blockade of TAK1 triggers caspase-8-dependent cleavage of gasdermin D and cell death. *Science* **362**, 1064-1069 (2018).

41. Kovacs SB*, et al.* Neutrophil Caspase-11 Is Essential to Defend against a Cytosol-Invasive Bacterium. *Cell Rep* **32**, 107967 (2020).

42. Franchi L, Stoolman J, Kanneganti TD, Verma A, Ramphal R, Nunez G. Critical role for Ipaf in Pseudomonas aeruginosa-induced caspase-1 activation. *Eur J Immunol* **37**, 3030-3039 (2007).

43. Boucher D*, et al.* Caspase-1 self-cleavage is an intrinsic mechanism to terminate inflammasome activity. *J Exp Med* **215**, 827-840 (2018).

44. Booshehri LM, Hoffman HM. CAPS and NLRP3. *J Clin Immunol* **39**, 277-286 (2019).

45. Stackowicz J*, et al.* Neutrophil-specific gain-of-function mutations in Nlrp3 promote development of cryopyrin-associated periodic syndrome. *J Exp Med* **218**, (2021).

46. Song N*, et al.* NLRP3 Phosphorylation Is an Essential Priming Event for Inflammasome Activation. *Mol Cell* **68**, 185-197 e186 (2017).

47. Liang Z, Damianou A, Di Daniel E, Kessler BM. Inflammasome activation controlled by the interplay between post-translational modifications: emerging drug target opportunities. *Cell Commun Signal* **19**, 23 (2021).

48. Zangiabadi S, Abdul-Sater AA. Regulation of the NLRP3 Inflammasome by Posttranslational Modifications. *J Immunol* **208**, 286-292 (2022).

49. Bose S, Segovia JA, Somarajan SR, Chang TH, Kannan TR, Baseman JB. ADP-ribosylation of NLRP3 by Mycoplasma pneumoniae CARDS toxin regulates inflammasome activity. *mBio* **5**, (2014).

50. Segovia JA*, et al.* NLRP3 Is a Critical Regulator of Inflammation and Innate Immune Cell Response during Mycoplasma pneumoniae Infection. *Infect Immun* **86**, (2018).

51. Lin AE*, et al.* A group A Streptococcus ADP-ribosyltransferase toxin stimulates a protective interleukin 1beta-dependent macrophage immune response. *mBio* **6**, e00133 (2015).

52. Bardet J*, et al.* NLRC4 GOF Mutations, a Challenging Diagnosis from Neonatal Age to Adulthood. *J Clin Med* **10**, (2021).

53. Canna SW*, et al.* An activating NLRC4 inflammasome mutation causes autoinflammation with recurrent macrophage activation syndrome. *Nat Genet* **46**, 1140-1146 (2014).

54. Kroken AR*, et al.* Exotoxin S secreted by internalized Pseudomonas aeruginosa delays lytic host cell death. *PLoS Pathog* **18**, e1010306 (2022).

55. Amara N*, et al.* Selective activation of PFKL suppresses the phagocytic oxidative burst. *Cell* **184**, 4480-4494 e4415 (2021).

56. Rietsch A, Mekalanos JJ. Metabolic regulation of type III secretion gene expression in Pseudomonas aeruginosa. *Mol Microbiol* **59**, 807-820 (2006).

Figure legends

Figure 1. GSDMD and *P. aeruginosa* T3SS dependent IL-1β secretion and pyroptosis in neutrophils. A. *P. aeruginosa* T3SS is preassembled and spans the bacterial cell envelope (IM, inner membrane, OM, outer membrane and PG, peptidoglycan layer). Following cell contact, the pore-forming translocator proteins, PopB (B) and PopD (D), assemble into a pore, which then docks to the needle tip (PcrV, red). Effector secretion is triggered, resulting in export of effector proteins across the bacterial cell envelope and host cell plasma membrane (PM) into the cytosol of the targeted cell. *P. aeruginosa* strain PAO1 used in the current study expresses ExoS, ExoT, and ExoY, but not ExoU. **B.** IL-1β cleavage in combined supernatants and lysates of bone marrow neutrophils from C57BL/6 mice primed 3h with LPS and incubated 45 min with ATP or with *P. aeruginosa* strain PAO1 or PAO1 mutants Δ*pscD* (no needle), Δ*popB* (no translocon), Δ*exoSTY* or Δ*exoST.* **C,D.** Quantification of IL-1β (**C**), and pyroptosis (lactate dehydrogenase, LDH, release, **D**). **E,F.** GSDMD, caspase-3 and GSDME cleavage in neutrophils and bone marrow derived macrophages incubated with extrinsic activators of apoptosis TNFα and SMAC mimetics (**TNF/SM),** with LPS alone, or LPS and PAO1 together with the ZVAD pan-caspase inhibitor or cycloheximide (CHX). **D-G.** IL-1β secretion and LDH release by neutrophils **(D,E)** or macrophages **(F,G)** from C57BL/6, *gsdmd*$^{-/-}$ *gsdme*$^{-/-}$ and *gsdmd/gsdme* $^{-/-}$ mice incubated with PAO1, Δ*pscD* or Δ*exoST* mutant bacteria. Each data point represents an independent biological repeat experiment Statistical significance was assessed by 2-way ANOVA followed by Tukey's post hoc analysis. Western blots are representative of 3 repeat experiments.

Figure 2. **Distinct roles for NLRC4 and T3SS exoenzymes in IL-1β secretion by macrophages compared with neutrophils**. **A,B.** IL-1β secretion by C57BL/6 and NLRC4$^{-/-}$ bone marrow derived macrophages and bone marrow neutrophils from mice incubated with PAO1, Δ*pscD* (no needle), Δ*popB* (no translocon), or Δ*exoST.* **C,D.** LDH release by

macrophages and neutrophils. **E,F.** Western blot showing GSDMD and IL-1β cleavage in macrophages (**E**) and neutrophils (**F**). Each data point represents an independent experiment. Statistical significance was assessed by 2-way ANOVA followed by Tukey's post hoc analysis. Western blots are representative of 3 repeat experiments.

Figure 3. **Distinct roles for NLRP3 and T3SS exoenzymes in IL-1β secretion by neutrophils compared with macrophages**. **A,B.** IL-1β secretion by C57BL/6 and NLRP3$^{-/-}$ bone marrow derived macrophages and bone marrow neutrophils from mice incubated with PAO1, Δ*pscD* (no needle), Δ*popB* (no translocon), or Δ*exoST.* **C,D.** LDH release by macrophages and neutrophils. **E,F.** GSDMD and IL-1β cleavage in neutrophils from C57BL/6 or NLRP3$^{-/-}$ mice infected with PAO1 or T3SS mutant bacteria **(E),** or in C57BL/6 neutrophils incubated with PAO1 or T3SS mutant bacteria together with the NLRP3 inhibitor MCC950 (**F**). **G.** GTPase (GAP) and ADP ribosyltransferase (ADPRT) regions of ExoS and ExoT showing amino acids required for enzymatic function and which are also the sites of point mutations. **H,I.** IL-1β secretion and LDH release by neutrophils from C57BL/6 mice stimulated with mutant bacteria with the exoenzyme mutants or bacteria with the indicated ExoS or ExoT point mutations (A-, G-). Strains that can inject ExoS ADPRT into host cells are indicated. Each data point represents the mean of independent repeat experiments. Statistical significance was assessed by 2-way ANOVA and Tukey's post hoc analysis. Western blots are representative of 3 repeat experiments.

Figure 4. ***P. aeruginosa* - induced neutrophil extracellular trap formation**. **A-C.** extracellular DNA quantified by Sytox™ green in human neutrophils incubated 16h with PMA, PAO1 or Δ*pscD* and the NADPH oxidase inhibitor DPI. Representative time courses (**A,B)** and area under the curve (AUC) for repeat experiments (**C**). **D-F.** Extracellular DNA release by

peritoneal neutrophils from C57BL/6 and *gsdmd*$^{-/-}$ mice incubated 16h with the same stimuli. Representative time course (**D,E)** and area under the curve (AUC) for repeat experiments (**F**). **G.** IL-1β secretion by peritoneal neutrophils from C57BL/6 mice primed 3h with LPS and 1h with ATP or PAO1 in the presence of necrosulfonamide (NSA), disulfiram or LDC7559. **H.** Extracellular DNA release from peritoneal neutrophils from C57BL/6 mice incubated 16h with PMA or PAO1 and GSDMD inhibitors. **I,J.** Extracellular DNA release in neutrophils from C57BL/6 and GSDME$^{-/-}$ mice incubated 16h with PMA or PAO1. Representative time course (**I)** and area under the curve (AUC) for repeat experiments (**J**). **K,L.** Citrullinated histone 3 (H3Cit) and DAPI staining of neutrophils from C57BL/6 or GSDMD$^{-/-}$ mice stimulated 16h with PAO1 or PMA. Representative images (**K)** and quantification **(L)** of H3Cit+ neutrophils per high power field. (Representative low power fields are shown in **Figure S1B**). Time course graphs of SYTOX release are representative experiments. Data points represent independent biological repeat experiments. Statistical significance was assessed by 2-way ANOVA and Tukey's post hoc analysis.

Figure 5. ***P. aeruginosa* corneal infection**. **A.** GSDMD, GSDME and IL-1β cleavage in PAO1 infected corneas of C57BL/6 or GSDMD/E$^{-/-}$ mice 24h post inoculation with 1 x 10^5 bacteria. **B**. IL-1β in infected C57BL/6 and GSDMD$^{-/-}$ corneas; **C,D.** Colony forming units (CFU) in C57BL/6 and GSDMD/E$^{-/-}$ eyes 48 post infection. Each data point represents an infected cornea and combines data from multiple experiments. **Inoc**: inoculum (CFU) in corneas 2h post-infection. Students t tests were used to assess statistical significance. Western blot is representative of two repeat experiments. Corneal disease and neutrophil infiltration data are in Figure S2.

Figure 6. Proposed sequence of events (see text for details)

Supplementary Figures

Figure S1. Role of GSDMD in ROS production and NETosis.

A,B. Reactive oxygen production by peritoneal neutrophils from C57BL/6 or GSDMD$^{-/-}$ mice incubated 90 min with PMA, PAO1 or Δ*pscD* in the presence of Luminol. **A.** Representative time course of relative luminescent units (RLU). **B.** Combined data from multiple experiments showing area under the curve.

C. H3Cit in neutrophils from C57BL/6 or GSDMD$^{-/-}$ mice incubated 16h with PMA or PAO1. Images shown in **Figure 4K** are a higher magnification of the inset boxes of PAO1 infected neutrophils.

Figure S2. Role of GSDMD and GSDME in PAO1 corneal infection.

A-E. Corneal infection in C57BL/6 and GSDMD$^{-/-}$ mice. Representative images of corneal opacification (bright field) and GFP expressing PAO1 24h and 48h post-infection of corneas of C57BL/6 and GSDMD$^{-/-}$ mice (**A**). **B.** Corneal opacification quantified by image analysis. **C.** GFP intensity quantified by image analysis. **D.** Representative flow cytometry scatter plots of PAO1 infected corneas of C57BL/6 and GSDMD$^{-/-}$ mice 24h post infection. Total cells were gated on live single cells. Neutrophils are Ly6G+ / CD11b+ whereas monocytes are Ly6G- / CD11b+. **E.** Total neutrophils in infected corneas quantified by flow cytometry (four repeat experiments).

E, F. Corneal infection in C57BL/6, GSDMD-/- and GSDMD/E$^{-/-}$ mice. E. Representative corneas of naïve mice or 24h post infection with PAO1 in C57BL/6 and GSDMD/E$^{-/-}$ mice. **F.** Quantification of corneal opacification by image analysis. Corneal images are x20 magnification; Each data point represents a single cornea, and data are combined from multiple experiments.

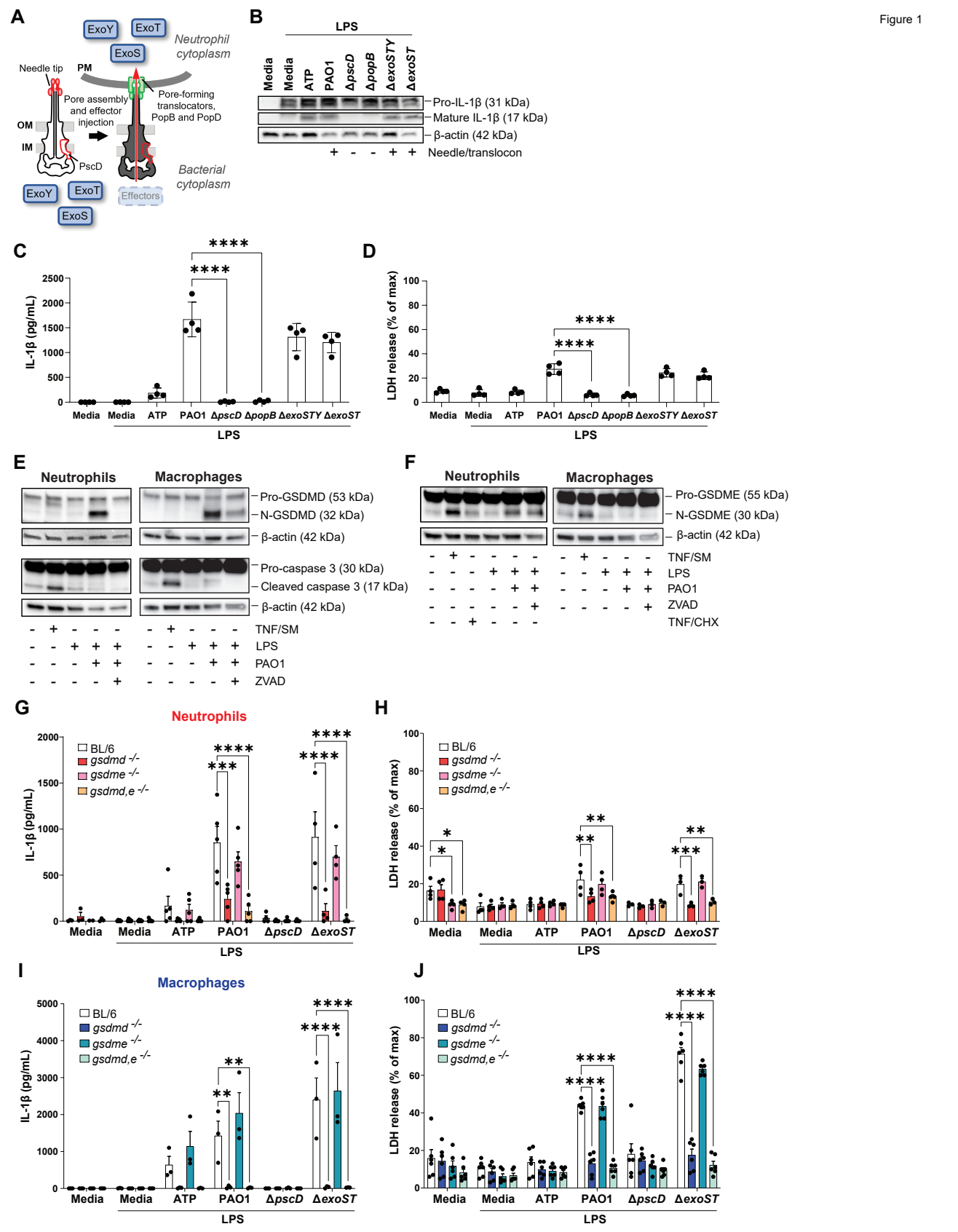
A
ExoY
ExoT
ExoS
Neutrophil cytoplasm
Needle tip
PM
Pore assembly and effector injection
Pore-forming translocators, PopB and PopD
OM
IM
PscD
Bacterial cytoplasm
Effectors
B
LPS
Media
Media
ATP
PAO1
ΔpscD
ΔpopB
ΔexoSTY
ΔexoST
Pro-IL-1β (31 kDa)
Mature IL-1β (17 kDa)
β-actin (42 kDa)
+ - - + + Needle/translocon
C
IL-1β (pg/mL)
D
LDH release (% of max)
LPS
E
Neutrophils
Macrophages
Pro-GSDMD (53 kDa)
N-GSDMD (32 kDa)
β-actin (42 kDa)
Pro-caspase 3 (30 kDa)
Cleaved caspase 3 (17 kDa)
TNF/SM
LPS
PAO1
ZVAD
F
Pro-GSDME (55 kDa)
N-GSDME (30 kDa)
TNF/CHX
G
Neutrophils
BL/6
gsdmd -/-
gsdme -/-
gsdmd,e -/-
H
I
Macrophages
J

Figure 2

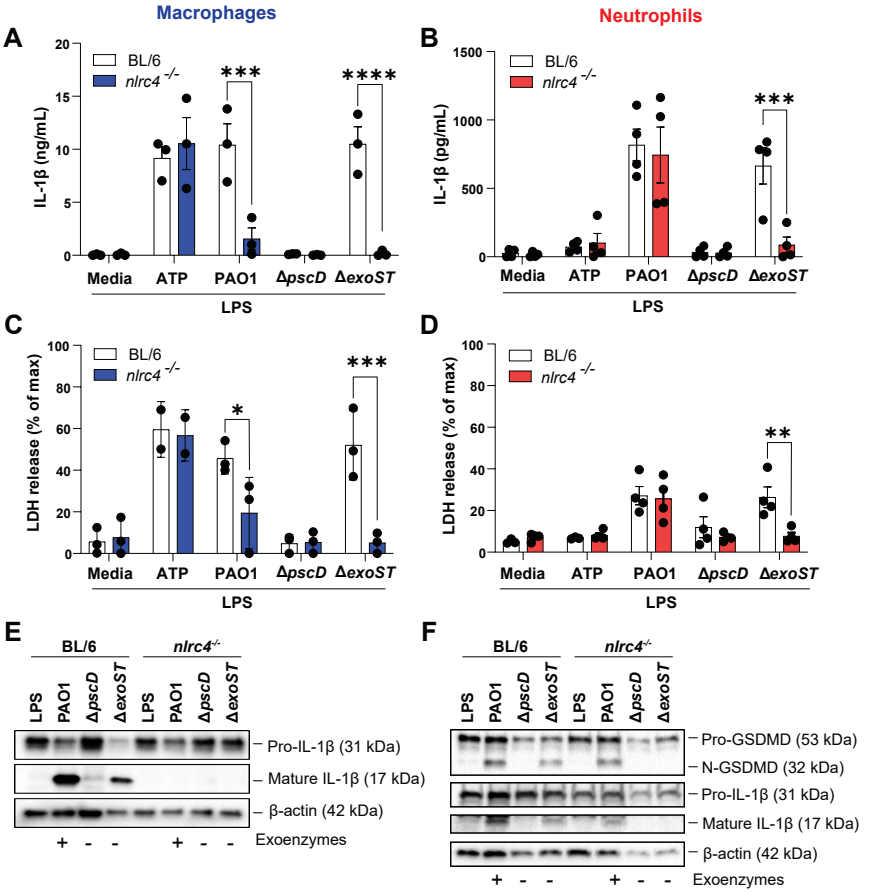
Macrophages
Neutrophils
A
B
C
D
E
F
BL/6
nlrc4 -/-
IL-1β (ng/mL)
IL-1β (pg/mL)
LDH release (% of max)
Media
ATP
PAO1
ΔpscD
ΔexoST
LPS
***
****
*
**
Pro-IL-1β (31 kDa)
Mature IL-1β (17 kDa)
β-actin (42 kDa)
Pro-GSDMD (53 kDa)
N-GSDMD (32 kDa)
Exoenzymes

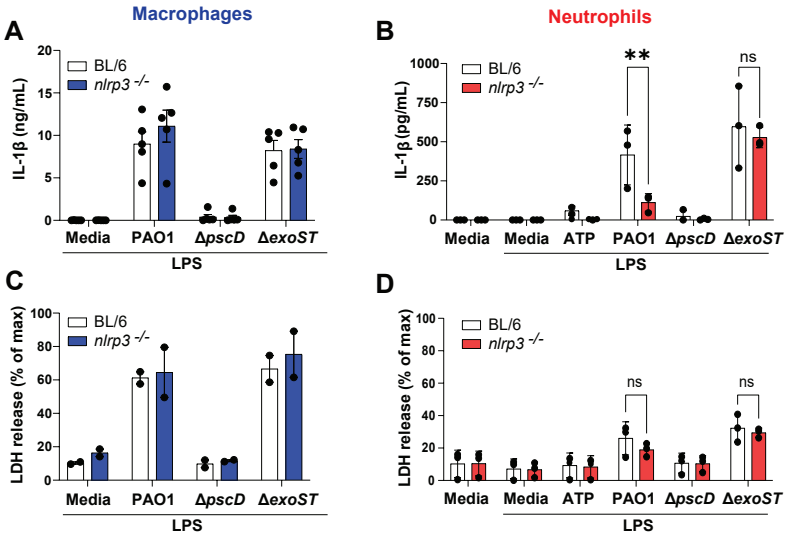
A
Macrophages
BL/6
nlrp3 -/-
IL-1β (ng/mL)
Media
PAO1
ΔpscD
ΔexoST
LPS
B
Neutrophils
BL/6
nlrp3 -/-
IL-1β (pg/mL)
**
ns
Media
Media
ATP
PAO1
ΔpscD
ΔexoST
LPS
C
BL/6
nlrp3 -/-
LDH release (% of max)
Media
PAO1
ΔpscD
ΔexoST
LPS
D
BL/6
nlrp3 -/-
LDH release (% of max)
ns
ns
Media
Media
ATP
PAO1
ΔpscD
ΔexoST
LPS

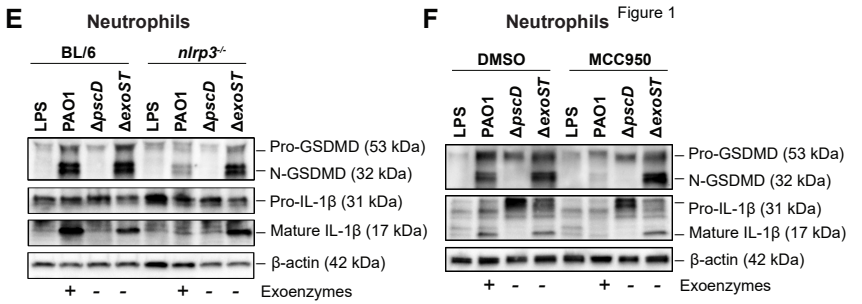
E
Neutrophils
BL/6
nlrp3-/-
LPS
PAO1
ΔpscD
ΔexoST
LPS
PAO1
ΔpscD
ΔexoST
Pro-GSDMD (53 kDa)
N-GSDMD (32 kDa)
Pro-IL-1β (31 kDa)
Mature IL-1β (17 kDa)
β-actin (42 kDa)
+ - - + - -
Exoenzymes
F
Neutrophils
DMSO
MCC950
LPS
PAO1
ΔpscD
ΔexoST
LPS
PAO1
ΔpscD
ΔexoST
Pro-GSDMD (53 kDa)
N-GSDMD (32 kDa)
Pro-IL-1β (31 kDa)
Mature IL-1β (17 kDa)
β-actin (42 kDa)
+ - - + - -
Exoenzymes

Figure 1

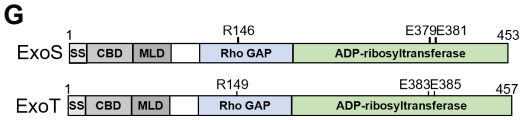
G
ExoS
1
SS
CBD
MLD
R146
Rho GAP
E379E381
ADP-ribosyltransferase
453
ExoT
1
SS
CBD
MLD
R149
Rho GAP
E383E385
ADP-ribosyltransferase
457

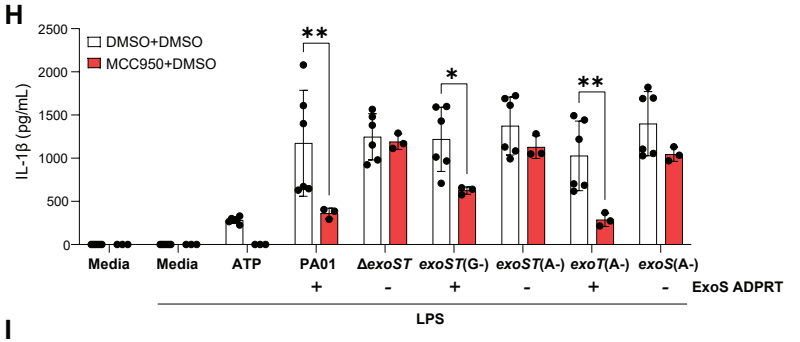
H
DMSO+DMSO
MCC950+DMSO
IL-1β (pg/mL)
**
*
**
Media
Media
ATP
PA01
ΔexoST
exoST(G-)
exoST(A-)
exoT(A-)
exoS(A-)
+ - + - + -
ExoS ADPRT
LPS

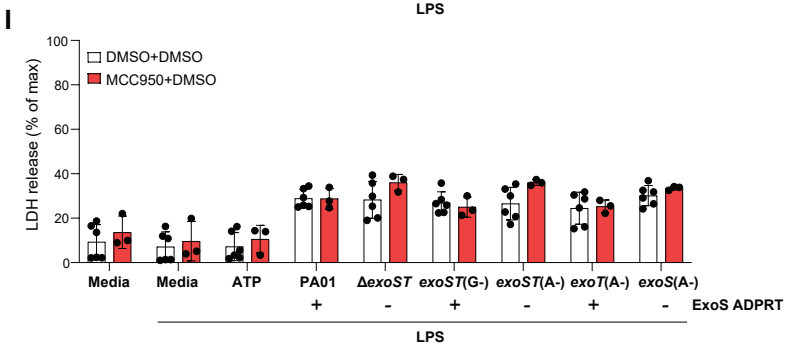
I
DMSO+DMSO
MCC950+DMSO
LDH release (% of max)
Media
Media
ATP
PA01
ΔexoST
exoST(G-)
exoST(A-)
exoT(A-)
exoS(A-)
+ - + - + -
ExoS ADPRT
LPS

Figure 4

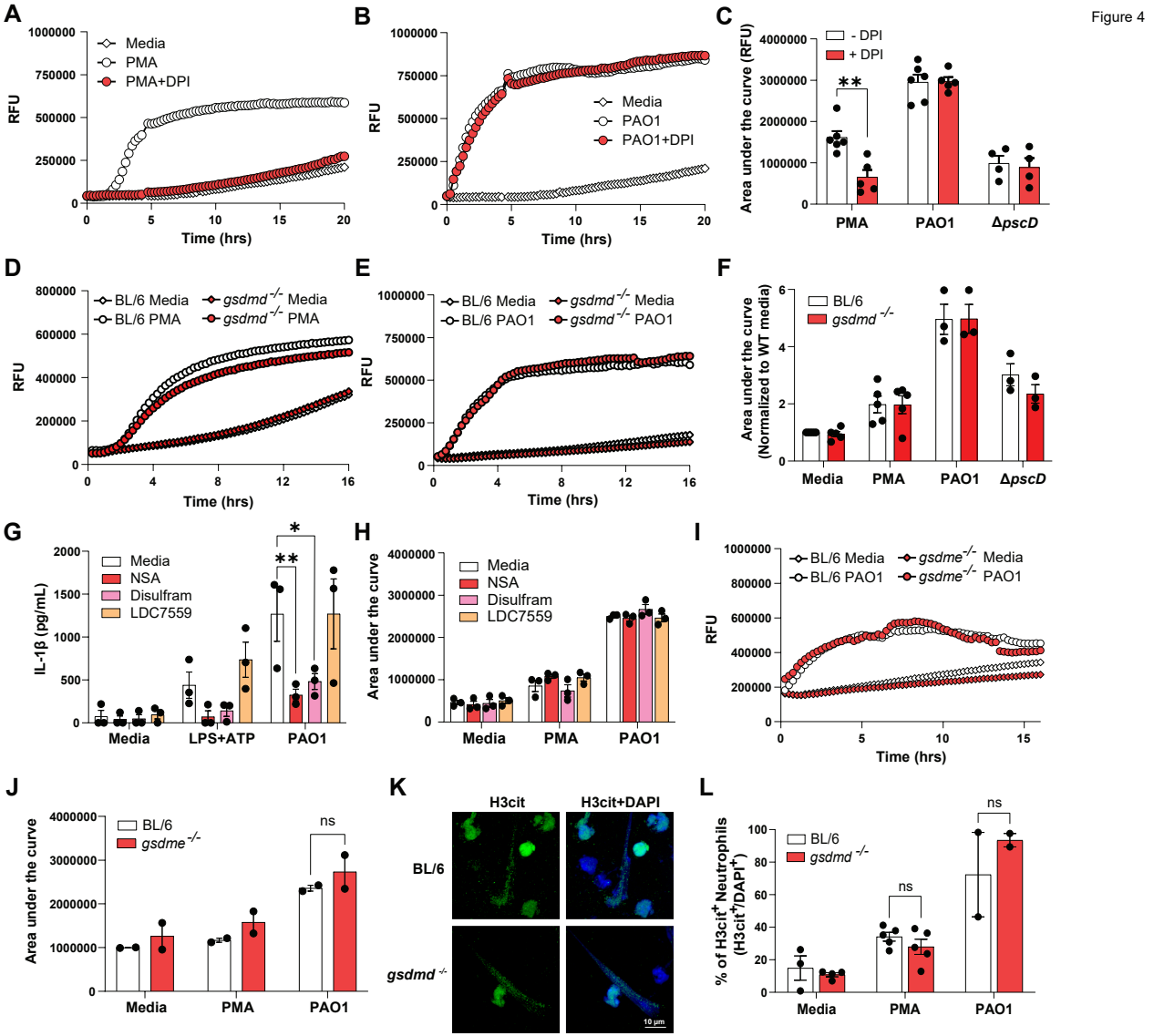
A
RFU
Time (hrs)
Media
PMA
PMA+DPI
B
RFU
Time (hrs)
Media
PAO1
PAO1+DPI
C
Area under the curve (RFU)
- DPI
+ DPI
**
PMA
PAO1
ΔpscD
D
RFU
Time (hrs)
BL/6 Media
BL/6 PMA
gsdmd -/- Media
gsdmd -/- PMA
E
RFU
Time (hrs)
BL/6 Media
BL/6 PAO1
gsdmd -/- Media
gsdmd -/- PAO1
F
Area under the curve (Normalized to WT media)
BL/6
gsdmd -/-
Media
PMA
PAO1
ΔpscD
G
IL-1β (pg/mL)
Media
NSA
Disulfram
LDC7559
*
**
Media
LPS+ATP
PAO1
H
Area under the curve
Media
NSA
Disulfram
LDC7559
Media
PMA
PAO1
I
RFU
Time (hrs)
BL/6 Media
BL/6 PAO1
gsdme -/- Media
gsdme -/- PAO1
J
Area under the curve
BL/6
gsdme -/-
ns
Media
PMA
PAO1
K
H3cit
H3cit+DAPI
BL/6
gsdmd -/-
10 µm
L
% of H3cit+ Neutrophils (H3cit+/DAPI+)
BL/6
gsdmd -/-
ns
ns
Media
PMA
PAO1

Figure 5

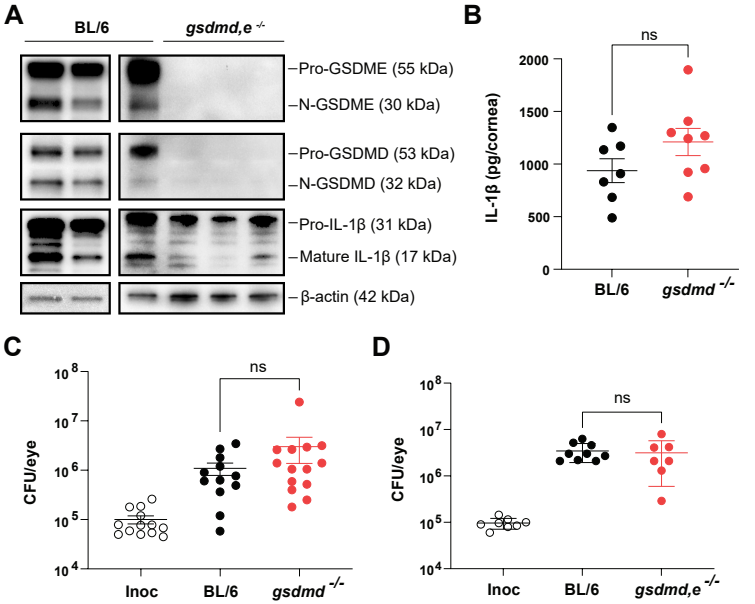
A
BL/6
gsdmd,e -/-
Pro-GSDME (55 kDa)
N-GSDME (30 kDa)
Pro-GSDMD (53 kDa)
N-GSDMD (32 kDa)
Pro-IL-1β (31 kDa)
Mature IL-1β (17 kDa)
β-actin (42 kDa)
B
ns
IL-1β (pg/cornea)
2000
1500
1000
500
0
BL/6
gsdmd -/-
C
ns
CFU/eye
10 8
10 7
10 6
10 5
10 4
Inoc
BL/6
gsdmd -/-
D
ns
CFU/eye
10 8
10 7
10 6
10 5
10 4
Inoc
BL/6
gsdmd,e -/-

Figure 6

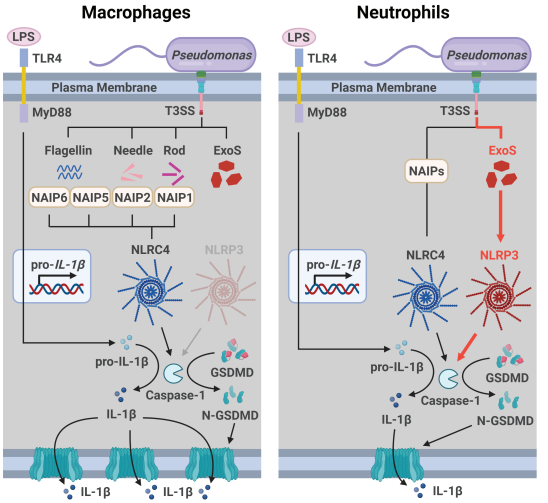
Macrophages
LPS
TLR4
Pseudomonas
Plasma Membrane
MyD88
T3SS
Flagellin
Needle
Rod
ExoS
NAIP6
NAIP5
NAIP2
NAIP1
pro-IL-1β
NLRC4
NLRP3
pro-IL-1β
GSDMD
Caspase-1
IL-1β
N-GSDMD
IL-1β
IL-1β
Neutrophils
LPS
TLR4
Pseudomonas
Plasma Membrane
MyD88
T3SS
ExoS
NAIPs
pro-IL-1β
NLRC4
NLRP3
pro-IL-1β
GSDMD
Caspase-1
IL-1β
N-GSDMD
IL-1β